ENVIRONMENT CANADA'S GEM (GLOBAL ENVIRONMENTAL MULTISCALE) MODEL

Andrew Staniforth, Jean Côté, Sylvie Gravel, André Méthot, Alain Patoine, and Michel Roch
Atmospheric Environment Service
Montreal, Canada

Summary: An operational integrated forecasting and data assimilation system has been and is continuing to be developed by the Atmospheric Environment Service of Environment Canada. The rationale for developing this system is given and the variable-resolution global model around which it is built is described. Some sample results are also presented.

1. INTRODUCTION

An integrated atmospheric environmental forecasting and simulation system, described herein, has been and is continuing to be developed by the Atmospheric Environment Service (AES) of Environment Canada. The bilingual acronym **GEM** has been adopted for the model around which this system is constructed. Thus in English the model is designated as "the **G**lobal **E**nvironmental **M**ultiscale model", whereas in French it is referred to as "le modèle **G**lobal **E**nvironnemental **M**ulti-échelle".

The goals of this paper are to:

- motivate and outline the development of a comprehensive global atmospheric environmental forecasting and simulation system;
- discuss various design considerations; and
- present some sample validation results.

2. RATIONALE FOR DEVELOPING A UNIVERSAL MODELING SYSTEM

Two operational data assimilation and weather forecasting cycles - one global and one regional - have been running daily at the Canadian Meteorological Centre (CMC) for a number of years. The global cycle, based on a spectral model (Ritchie and Beaudoin, 1994), addresses medium-range forecasting needs and global data assimilation. The regional cycle provides the more detailed short-range (to 2 days) forecasts over N. America and some of its adjacent waters, and was based on the Regional Finite Element (RFE) model (Mailhot et al. 1997) until its recent replacement by the GEM model.

Even though the two-cycle strategy is a costly choice, it is considered the only acceptable alternative for fulfilling the operational needs for *both* medium-range (and therefore necessarily global) forecasting, and high-resolution regional forecasting. If the two cycles are centered around two distinct models, the strategy then requires the maintenance, improvement and optimization of two sets of libraries and procedures. This is very labor intensive (Courtier et al., 1991; Cullen, 1993; Côté et al., 1993), and is so for principally three reasons. First, numerical-weather-prediction models and data assimilation systems need significant recoding in order to reap the benefits afforded by the new high-performance significantly-parallel computer platforms. Second, to improve the accuracy of the initial state of the atmosphere, i.e. that of the analysis, requires a significant investment in the research and development of new data assimilation methods. Third, to improve the predictive capability of a weather forecast model requires a significant effort to be devoted to the improvement of model parameterizations. These motivate the consolidation of both the global and regional assimilation and forecasting systems within a single flexible modelling framework.

This was thus the main incentive for the development of the GEM model. Using similar reasoning, both Météo France (Courtier et al., 1991) and the U.K. Meteorological Office (Cullen, 1993) have developed unification strategies, which are however different. At Météo France, the IFS/ ARPEGE/ ALADIN (Integrated Forecast System/ Action de Recherche Petite Échelle Grande Échelle/ Aire Limitée Adaptation Dynamique Développement InterNational) forecast system has been developed in collaboration with the ECMWF (European Centre for Medium-range Weather Forecasts). It is based on the use of a global variable-resolution spectral model as proposed in Courtier and Geleyn (1988). For medium-range applications the system is run at uniform resolution by ECMWF, whereas it is run by Météo France with variable-resolution concentrated over France for regional forecasts to 3 days (Yessad and Bénard, 1996). Because of some unanticipated intrinsic limitations on resolution (Caian and Geleyn, 1997) due to the use of the Schmidt (1977) coordinate transformation to achieve variable resolution with a spectral model, a limited-area nonhydrostatic version (ALADIN) has been developed (Bubnova et al., 1995) for higher and more-focused resolution applications using code shared with that of the global version.

The strategy of the UKMO is both similar and different. It uses the UKMO's global uniform-resolution finite-difference Unified forecast/ climate model (Cullen, 1993; Cullen et al., 1997) for medium-range forecasting and climate simulation, and a limited-area code-shared version for mesoscale forecasting. In the context of medium-range forecasting and climate simulation, Cullen (1993) remarked that "Maintenance of two separate systems is no longer practicable or justified". In the context of medium-range and mesoscale forecasting he further noted that the unified strategy "... avoids the need for two separate teams of scientists and software systems, and allows the techniques used in large-scale modelling to be rigorously tested at the higher resolution used in the mesoscale model against the detailed observations available over the United Kingdom". It also ensures a certain consistency between the driven and driving models regarding the numerical methods and parameterizations used, inasmuch as there is much communality for these latter between the two configurations.

Our own unification strategy is based on the global variable-resolution strategy outlined in the shallow-water proof-of-concept work of Côté et al. (1993). As mentioned therein, the adopted strategy was influenced by the Courtier and Geleyn (1988) work but is, as argued both in Côté et al. (1993) and below, more flexible and of broader application.

The foregoing motivates the development of a new highly-flexible modelling system capable of meeting the weather-forecasting needs, both operational and research, of Canada for the coming years. Such a modelling system also has the potential to meet those of air quality and climate modelling. As indicated in Cullen (1993), there are advantages of doing weather-forecasting and climate modelling within a single universal model framework. It is obviously more economical to maintain and further develop a single model than two or more. Furthermore, any improvements developed for weather forecasting or for climate simulation, are immediately available for other applications, and improved validation of parameterizations is possible because they can be easily tested in both weather forecasting and climate mode. Validation in climate mode reduces the likelihood of a climate drift when a parameterization is used in a data-assimilation cycle, whereas running in weather-forecast

mode provides a better validation of the physical fidelity of certain parameterizations because of a more direct comparison against observations with much less spatio-temporal averaging of the verification data.

A discussion follows of some of the more important design considerations for the GEM model at the heart of this modelling system.

3. VARIABLE HORIZONTAL RESOLUTION

3.1 Rationale for global variable resolution

The compromise of regional modelling is to favour high local resolution at the expense of a reduced period of validity. To protect the integrity of a forecast over an area of interest throughout the forecast period requires a computational domain much larger than the area of interest, since poorly-resolved features at and near the computational boundaries propagate inwards and contaminate the forecast, resulting in an ever-diminishing sub-domain over which the forecast is accurate. Even under the most favorable circumstances errors will be advected inwards by the local wind. As a minimum, the uniform-resolution part of any computational domain therefore has to be sufficiently large that the entire embedded area of interest will not be contaminated at any time during the integration period by any error advected inwards from its boundary. Also any resolution degradation or any application of numerical artifices such as blending or enhanced diffusion, should only be applied outside this pristine uniform-resolution part of the computational domain. Generally, the longer the integration time and the larger the area of interest, the larger must be the pristine uniform-resolution computational domain within which the area of interest is embedded.

Strategies for regional modelling fall into two broad classes: interactive and non-interactive (e.g. Anthes, 1983; Arakawa, 1984; Staniforth, 1997). For the *non-interactive* approach (the most popular one) a coarse-resolution forecast is used to specify time-dependent lateral boundary conditions for a model integrated over a limited area. The principal difficulty with this approach is the proper specification of lateral boundary conditions for open domains, and is related to fundamental problems of mathematical well-posedness (Oliger and Sundström, 1978). It is theoretically possible to obtain a well-posed problem with a point-wise specification of boundary conditions for the *continuously*-defined Euler equations, but *not* for the hydrostatic primitive equations. However most if not all limited-area models *overspecify* these conditions, regardless of which particular equation set (hydrostatic primitive, nonhydrostatic Euler, or anelastic) is employed, thereby leading to an ill-posed *discrete* problem. In the absence of any control mechanism this usually leads to noise at the smallest-resolvable scale, which often appears near outflow boundaries and then spuriously propagates upstream (e.g. Arakawa, 1984; Robert and Yakimiw, 1986). To compound the problem, spatial computational solutions can under certain circumstances be spuriously forced by lateral boundary conditions (Mesinger 1973).

A practical acid test that any successful limited-area model should meet (Yakimiw and Robert, 1990) is that *the solution obtained over a limited area should well match that of an equivalent-resolution model integrated over a much-larger domain.* It is surprisingly difficult to meet this acid test even under very simple conditions. Motivated by the failure of a baroclinic limited-area model undergoing validation tests to satisfy this criterion, Robert and Yakimiw (1986) evaluated, in the context of the linearized 1-d shallow-water equations, three

nesting strategies, variants of which are still used in almost all of today's limited-area models. They found that none of these methods works acceptably well for this simple problem.

There have been a number of other reports over the years, both theoretical and practical, concerning lateral-boundary-condition-related difficulties with the non-interactive approach. In our opinion, the problems of specifying and applying lateral boundary conditions for limited-area models have not as yet been entirely resolved, and more needs to be done to validate the methodologies employed by today's mesoscale models, both interactive and non-interactive. A tangent linear model of a forecast model provides a powerful evaluation tool in this regard (Errico et al., 1993).

Our own preference for strategy is the *interactive* approach (e.g. Harrison and Elsberry, 1972; Phillips and Shukla, 1973; Kurihara and Tuleya, 1974; Courtier and Geleyn, 1988) where the resolution is varied in some manner away from the fine resolution of an area of interest to the coarser resolution of a surrounding outer region. Arakawa (1984) claims that this approach is conceptually superior. It has the desirable features that the flows inside and outside the area of interest mutually interact in a single dynamic system, and that it addresses the well-posedness issue of limited-area models. This is accomplished at the cost of integrating over a larger domain, usually taken to be either quasi-hemispheric or global. The cost-effectiveness of this is discussed further below. A smooth degradation of resolution in the outer domain avoids the deleterious impact on the accuracy of the solution of an abrupt change in resolution (Arakawa, 1984; Fox-Rabinovitz et al., 1997). The results of Gravel and Staniforth (1992) indicate that even if the resolution can be varied abruptly without introducing significant noise, the accuracy of the solution can nevertheless be severely and unacceptably degraded.

3.2 Different approaches to global variable-resolution

Variable resolution over the globe can be achieved in a number of different ways. In Courtier and Geleyn (1988) and Hardiker (1997) a continuous coordinate mapping due to Schmidt (1977) is employed such that the efficiency of the spectral method is hardly affected, and this approach is used in Météo France's operational ARPEGE model (Courtier et al., 1991). However the nature of the conformal coordinate transformation limits the focusing of the resolution to, roughly-speaking, meso-β-scale applications (Caian and Geleyn, 1997). A different continuous coordinate mapping, which is weakly-varying and orthogonal but non-conformal, is used in Sharma et al. (1987) in the context of a finite-difference discretization. In Paegle (1989), Paegle et al. (1997) and Côté et al. (1993), variable resolution is achieved using finite elements. For the Paegle et al. (1989, 1997) formulation the resolution is varied and focused in the North-South coordinate direction only.

The Côté et al. (1993) formulation adopted here is more general, and it permits resolution to be simultaneously varied in both coordinate directions in a flexible manner. It uses a regular (but variable-resolution) arbitrarily-rotated lat-lon mesh. The regular lat-lon mesh facilitates computational efficiency since its regularity is reflected in the resulting matrix structures, and certain properties that only hold for regular meshes can then be exploited (see Staniforth, 1987, for discussion). Rotating the mesh permits resolution to be focused over any area on the earth. Sufficiently far-removed from the uniform-resolution subdomain, the variable-resolution forecast will of

course be of inferior quality to that of a uniform-resolution medium-range one, and this is only to be expected. It is simply the result of trading enhanced accuracy over a region of interest against reduced accuracy (or no forecast at all) elsewhere, and it is the essence of all regional forecasting strategies.

Variable resolution gives rise to a local degradation in accuracy and this results in local flow distortions. This distortion is however quite small in regions where the resolution is not significantly degraded. Kalnay de Rivas (1972) and Fox-Rabinovitz et al. (1997) have examined the truncation errors associated with the approximation of derivatives on a variable-resolution mesh. They show that approximating derivatives on non-uniform but smoothly-varying meshes such as those described herein can be considered to be equivalent to approximating them with uniform-resolution in a transformed coordinate system. Smoothly varying the mesh has two advantages. First it keeps the local truncation errors reasonably small, although they are larger in the region of degraded resolution as one would expect. Second, compared to using meshes with an abrupt variation in resolution, spurious dispersion is greatly reduced as discussed in Fox-Rabinovitz et al. (1997) and in considerably-more detail in Vichnevetsky (1987). Smoothly varying the resolution greatly reduces the possibility that the group velocity spuriously changes sign, which is the mathematical criterion that determines whether wave reflection occurs or not. This makes it a lot less likely that gravitational disturbances propagating outwards from the uniform-resolution part of the domain will be spuriously reflected back from the internal boundary where resolution changes. Instead they continue outwards as they should, albeit with some flow distortion as they leave the uniform-resolution subdomain.

3.3 Different mesh configurations for different applications

For global-scale problems, such as medium-range, monthly, and seasonal weather forecasting, the long-range transport of pollutants, and climate scenarios, a uniform lat-lon mesh configuration is appropriate. Resolution can in principle be degraded somewhat in the southern hemisphere for some northern hemisphere applications, and vice versa. Fox-Rabinovitz et al. (1997) report success with this strategy for the Held and Suarez (1994) dynamic-core problem.

For smaller-scale problems, several variable-resolution horizontal mesh configurations are displayed in Figs. 1-3, illustrating the flexibility of the approach. The first of these, shown in Fig. 1, is suitable for forecasting at the synoptic scale for periods of up to 48 h. Over N. America the resolution is 0.33°, and the resolution smoothly degrades away from the uniform-resolution subdomain with each successive mesh-length being approximately 10% larger than that of its preceding neighbour. This mesh was used operationally from Feb 1997 - Sept 1998 (the model was then reconfigured to increase resolution over the uniform-resolution sub-domain to 0.22° whilst still smoothly varying the resolution in the same way). The uniformly-spaced (in latitude and longitude) meshpoints in the high-resolution window of Fig. 1 are also almost uniformly spaced on the sphere with mesh-lengths that vary between a maximum of approximately 37 km (for mesh-lengths oriented West to East) and a minimum of 29 km (attained on the Atlantic and Pacific boundaries). Although this is not an essential element of the strategy, it was found convenient to orient the GEM model's mesh as in Fig. 1 because it gives somewhat enhanced resolution at inflow on the western geographical boundary of the high-resolution window.

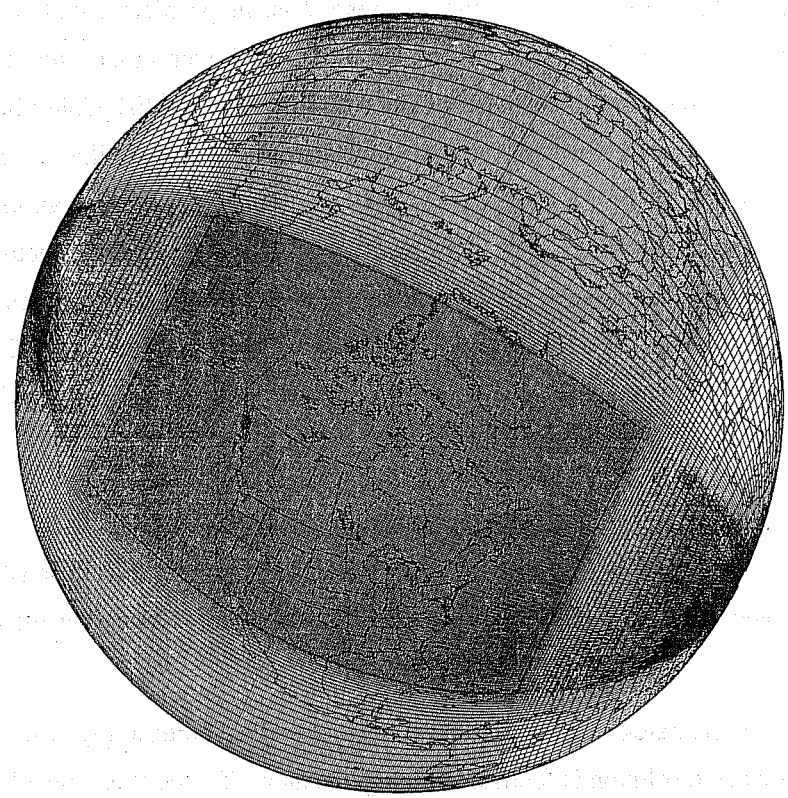

Fig. 1 The 255 x 289 variable-resolution horizontal grid of the initial operational regional configuration of the GEM model: it has uniform 0.33° resolution over the 59.07° x 77.22° (180 x 235) central window.

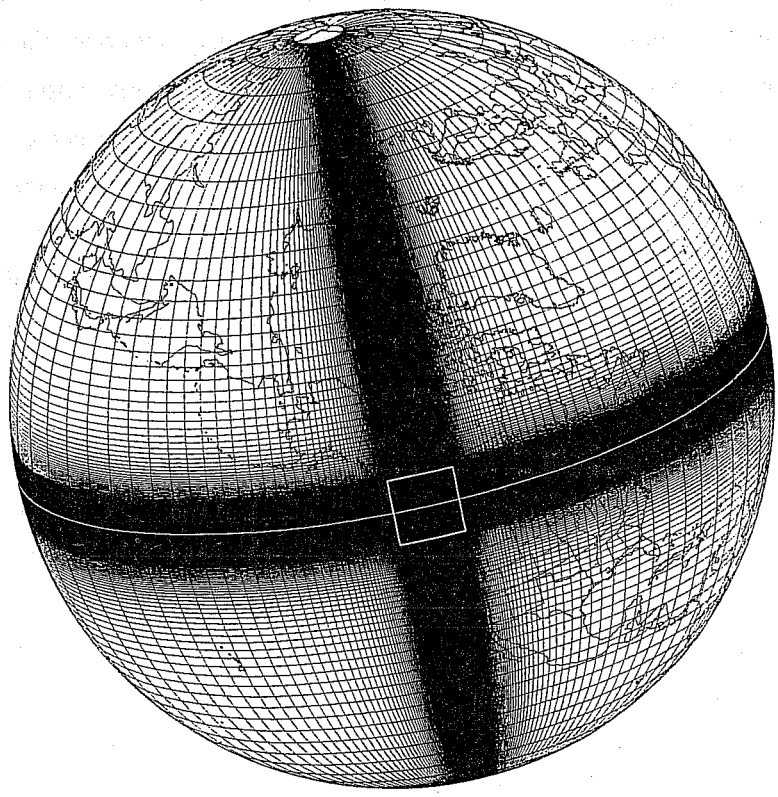

Fig. 2 A variable-resolution 427 x 414 *meso-*β mesh having a 10° x 10° (304 x 304) window of uniform 0.033° resolution, centred on (122°W, 53.5°N).

The second grid configuration (Fig. 2) is suitable for meso- β-scale problems, such as forecasting the weather in more detail for periods up to 12 h. The resolution is now focused over a much smaller-size (10° x 10° ~ 1100 km x 1100 km) uniform-resolution sub-domain, which is centered over British Columbia for this example. The resolution (0.033° ~ 3.6 km) of this subdomain is ten times finer than that of Fig. 1. The third grid configuration (Fig. 3) is suitable for meso- γ-scale problems, such as simulating an urban smog episode for a few hours, and the mesh is now centered over Montreal Island. For this highly-focused mesh, the resolution (0.0033° ~ 360 m) is further increased by a factor of ten and focused over a fifty-times-smaller (1.36° x 1.36° ~ 150 km x 150 km) sub-domain. For both the meso- β and meso- γ meshes (Figs. 2-3), the resolution again varies smoothly away from the uniform-resolution sub-domain, with the same approximately 10% successive increase in meshlength as the synoptic-scale configuration (Fig. 1).

3.4 Mesh properties

All three of the shown mesh configurations have the remarkable property that at least 50% of the total mesh points (i.e. approximately 70% for each of the two coordinate directions) are over the uniform high-resolution area of interest.

The adopted variable-mesh strategy has the property that it becomes increasingly cost-effective as a function of increasing resolution when resolution is focused over a given area. To see this, consider the cost of increasing the resolution over the uniform-resolution subdomain of the operational mesh (Fig. 1) while holding its size fixed, and while also smoothly degrading the resolution away from this subdomain in exactly the same manner: i.e. each successive meshlength is always approximately 10% larger than its predecessor when moving outwards in any of the four compass directions. The percentage of points over the uniform-resolution N. American subdomain then increases exponentially as a function of increasing resolution over the subdomain (see Fig. 4, obtained using the analysis given in Appendix A of Côté et al., 1998a). When computer power becomes available at the CMC to allow a 10-km-resolution regional configuration, the percentage of meshpoints over the subdomain of interest will go from the 65% (approximately 80% in each coordinate direction) of the current 0.22°-resolution operational mesh, to 78% (approximately 88% in each of the two directions). Thus this global variable-resolution strategy, which is already viable for regional forecasting for Canada at today's resolution, will become ever more so in the future.

3.5 Discussion

As stated above, global variable resolution has the desirable features that the flows inside and outside the area of interest mutually interact in a single dynamic system, and that it addresses the well-posedness issue of limited-area models. This is however accomplished at the cost of integrating over a larger domain and it is natural to ask the questions, how does the cost of running a variable-resolution global model compare to that of running a limited-area model, and what does one get for the expended computational effort? These are very difficult questions to answer in a general manner since the answers depend on many factors such as: the size and geographical location of the area of interest, the forecast period, the resolution, the prevailing meteorological conditions, the difference in resolution between driving and driven models, the accuracy of a driving model's

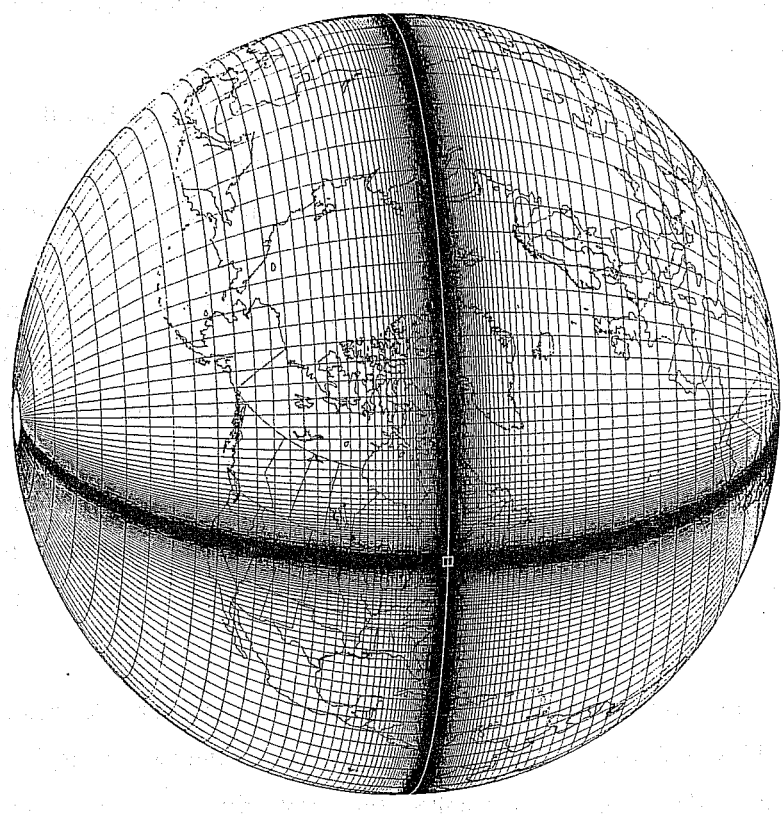

Fig. 3 A variable-resolution 584 x 569 *meso-*γ mesh having a 150 km x 150 km (413 x 413) window of uniform 0.0033° resolution, centred on (73.5°W, 45.5°N).

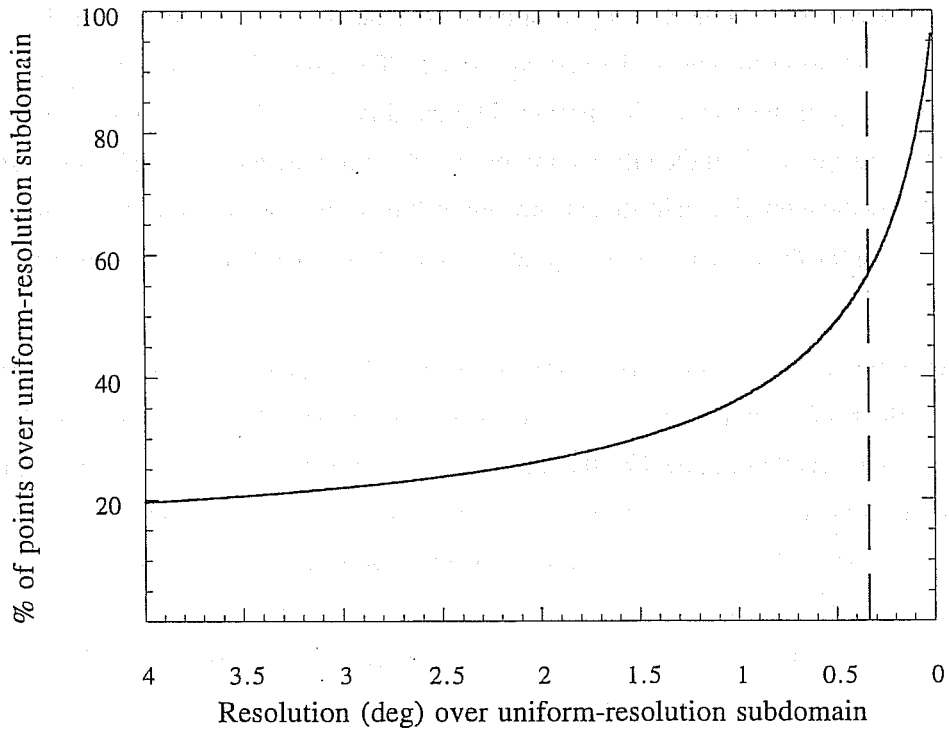

Fig. 4 The percentage of points located over the uniform-res 59.07° x 77.22° subdomain of the operational regional configuration of the GEM model w.r.t. the total no. of points, as a function of increasing resolution. Dashed line denotes the current operational resolution.

forecast, and the particular limited-area or variable-resolution techniques employed. Nevertheless, an attempt will be made to theoretically outline some of the issues.

Assume that it is desired to obtain a forecast over a specified area of interest, such as the U.S. or Canada, for a certain period of time, say 48 h, at a certain resolution. To guarantee the integrity of the forecast at this resolution at the end of the time period, it is necessary as a minimum to integrate a model over a larger region at the uniform high resolution of the now-embedded area of interest. No numerical "fixes" are allowed within this larger area since the resulting errors would have the time to contaminate the area of interest within the forecast period and compromise its integrity. As discussed in Staniforth (1997), the size of this uniform-resolution integration domain depends very much upon the period of integration, the size of the area of interest, and the meteorological conditions, but it is typically many times larger than the area of interest. This is particularly so for wintertime situations with strong jets, and much less so for summertime ones with weak synoptic circulations but strong sub-synoptic ones. Most forecast centers use a fixed integration area for all seasons, and it can be inferred from this that they intend that the chosen integration domain be able to properly handle worst-case scenarios.

Thus far in the argument, no distinction has been made between the global variable-resolution and limited-area strategies and, all other things being equal, the computational cost of the two strategies is thus far identical. Where things differ is how, and at what cost, one embeds this "protective" area within an even-larger integration domain. In a perfect world there would be no need to make this further extension of integration domain for the driven limited-area strategy, and it would be a clear winner. In reality, and as discussed above, it is necessary to enclose the minimum-sized "protective area" by a computational buffer region of sufficient size to adequately adjust the limited-area solution to that of the driving model. The size of this boundary region very much depends upon the accuracy of the information provided by the driving model within this region and upon the numerical adjustment strategy used. If the information provided is accurate and reasonably consistent with that of the driven model, and the numerical adjustment strategy well respects this (see however Staniforth, 1997, for a blending counter-example), then this helps to keep this region, and the overhead, small: otherwise it may need to be much larger.

For the variable-resolution strategy, additional meshpoints have to be added to provide global coverage, subject to the constraint that the resolution does not vary too rapidly. This overhead, which varies widely according to application, is in our view greatly mitigated by the fact that the approach leads to a mathematically well-posed problem, and therefore is more likely to robustly give good results over a broader spectrum of situations than the limited-area one. To establish the cost of the overhead would require a comparison with the cost of running both a limited-area model and its driving model. Unfortunately this is virtually impossible since there is no consensus in the community on the size of the computational buffer zone needed by the limited-area model, something which greatly influences the comparative cost of the two strategies. We believe that the required width of this buffer zone is often under-estimated, possibly seriously so. We also believe that a 10% local variation in meshlength is a conservative estimate which could conceivably be significantly increased when flow gradients are small around the uniform-resolution subdomain (e.g. for an idealized mesoscale simulation

embedded within a quiescent environment), with a consequent reduction in the overhead. The diffusion coefficient could also be increased outside of the uniform-resolution sub-domain to locally control any problems due to a more-rapid local variation of resolution.

4. OTHER NUMERICAL MODELLING DESIGN CONSIDERATIONS

4.1 Non-hydrostatic considerations

The hydrostatic assumption, viz. the neglect of vertical acceleration in the vertical momentum equation, is an excellent approximation that is well respected in the atmosphere down to scales of 10 km or so. However at these scales the dynamical effects excluded by the hydrostatic assumption, for example internal wave breaking and overturning, start to become non-negligible. To date, computer limitations have been such that almost all operational weather-forecast (and climate-simulation) models have been run with horizontal meshlengths coarse enough to confidently employ the hydrostatic primitive equations.

If the new model is to be applied with meso-γ-scale mesh configurations similar to that of Fig. 3, then it should use the fully-compressible Euler equations instead of the so-called hydrostatic primitive ones. This motivates the use of the "hydrostatic-pressure" vertical coordinate proposed in Laprise (1992). This coordinate system permits a switch-controlled choice between the hydrostatic primitive equations (for large- and synoptic-scale applications), and the non-hydrostatic Euler equations (for smaller-scale applications), thus getting the best of two worlds. The computational and memory overhead associated with the latter option can then be avoided for applications where the hydrostatic approximation is valid. A terrain-following normalized pressure (Phillips, 1957; Kasahara, 1974) version is possible (Bubnova et al., 1995), allowing an easy incorporation of the lower boundary, and a relaxation towards the horizontal upwards from the Earth's surface. For atmospheric applications, there is virtually no scale restriction on using hydrostatic pressure as vertical coordinate since it only requires density to be positive, and integrations are presented in Bubnova et al. (1995) with horizontal resolution as high as 80 m. Note however that terrain-following transformations ultimately break down in the presence of cliffs due to a breakdown of differentiability.

The vertical coordinate of the GEM model is defined by:

$$\eta = \frac{\pi - \pi_T}{\pi_S - \pi_T}, \tag{4.1}$$

where π is the "hydrostatic pressure" of Laprise, i.e. it satisfies

$$\rho g = -\frac{\partial \pi}{\partial z}. \tag{4.2}$$

It has the advantage that it permits a straightforward adaptation of an existing library of physical parameterizations developed over the last decade or so.

4.2 Efficient time integration schemes

Numerical efficiency is very important when modelling the atmosphere. Vertically-propagating acoustic waves and horizontally-propagating external gravity waves propagate many times faster than the local windspeed, by a factor three or more depending upon application. The timestep of explicit Eulerian integration schemes is

restricted by the speed of the fastest-propagating modes, which means that the timestep is usually constrained by modes which carry little energy. The restrictions are particularly severe for lat-lon global finite-difference or finite-element models due to the convergence of the meridians at the poles. This motivates the use of an implicit (or semi-implicit) time treatment of the terms that govern the propagation of acoustic and gravitational oscillations in order to greatly retard their propagation and permit a much larger timestep. It results in the need to solve a 3-d elliptic-boundary-value (ebv) problem. For a time-implicit scheme to be computationally advantageous, it must be possible to integrate with a sufficiently-large timestep to offset the overhead of solving the ebv problem. This is usually the case even for nonhydrostatic flows as discussed in Skamarock et al. (1997).

A further advantage of a time-implicit treatment of acoustic and gravitational oscillations (Staniforth, 1997) is that for large timesteps it dramatically retards the inward propagation of any error from the boundary region of a limited-area model, or from the outer region of a variable-resolution model. To protect the integrity of the forecast over an area of interest against contamination by any significant such source of error, a proportionately-larger and possibly prohibitively-costly computational domain would thus be needed by a model that employs an explicit time treatment of the acoustic and gravity terms.

For an Eulerian treatment of advection, the use of an implicit or semi-implicit time scheme then constrains the local Courant number ($U\Delta t / \Delta x$) to be somewhat less than unity. Again for a lat-lon representation of the sphere this is particularly restrictive in polar regions due to the convergence of the meridians, but elsewhere the time truncation error is still several factors smaller than the spatial truncation error. This motivates the use of a semi-Lagrangian treatment of advection (Robert, 1981, 1982; see Staniforth and Côté, 1991, for a review), which is stable for Courant numbers much greater than unity and permits the timestep to be chosen on the basis of accuracy rather than stability. The governing equations are thus approximated along a parcel trajectory that arrives at a meshpoint at the new timestep. The evaluation of substantive derivatives then reduces to taking a time difference along a trajectory. Upstream values are computed by interpolation (usually cubic) of values at meshpoints surrounding the departure point (which is generally not a meshpoint).

Semi-implicit semi-Lagrangian methods were originally developed for hydrostatic primitive equation models (Robert et al., 1985) and are finding increasing favour for both weather-forecast models and climate models, as discussed in Côté et al. (1998a). They have also been extended to the fully-compressible Euler equations (e.g. Tanguay et al., 1990; Bubnova et al., 1995; Semazzi et al., 1995; Cullen et al., 1997).

4.3 Monotonicity and conservation

The interpolation procedure of the semi-Lagrangian algorithm can give rise to a local violation of monotonicity due to the Gibbs phenomenon. This can have particularly deleterious effects for physical quantities used by either the subgrid-scale parameterization, or a chemical transport model. To alleviate this potential problem, the monotonic scheme of Bermejo and Staniforth (1992) is adopted. In this scheme, a high-order estimate (using cubic interpolation) is blended with a low-order one (using linear interpolation which guarantees monotonicity). Consistent with approximation theory, the blending is done in such a way that the high-order solution is

favoured whenever smoothness warrants it (i.e. most of the time), otherwise the low-order solution is more strongly weighted.

Conservation is considered by some to be a potential problem for semi-Lagrangian schemes. Although conservation is generally excellent for short-term high-resolution integrations, it may be inadequate for longer (climate-scale) simulations, or for particularly-sensitive air-quality studies. Priestley (1993) proposed a conserving variant of the monotonic Bermejo and Staniforth algorithm such that conservation is additionally enforced as a constraint via a minimization procedure, with local adjustements being made where the interpolation procedure is most susceptible to have introduced errors. This has been introduced into the GEM model as an option.

5. DATA ASSIMILATION

Assimilation of both in-situ and remotely-sensed data provides the initial conditions required for numerical weather prediction. Since numerical models are usually used as constraints for data assimilation, present and anticipated developments in data assimilation must be taken into account when designing a new model. A number of issues relevant to the development of data assimilation for the GEM model are now touched upon.

Considerations for assimilating data at large and synoptic scales using the GEM model with uniform resolution are very similar to those for global uniform-resolution gridpoint models. Additional problems are however generally encountered when assimilating data at higher resolution. Some of these are related to fundamental scale and data issues, whereas some are peculiar to which strategy (interactive or non-interactive) is adopted for regional modelling.

The advection of poorly-resolved information from outside a pristine uniform-resolution subdomain increases the forecast error of the model, be it interactive or non-interactive, used as a constraint in mesoscale data assimilation. For a limited-area model this is due to the lower space and time resolution of the driving model that furnishes the boundary conditions, and to the damping effect of the surrounding computational buffer region as information propagates through it. For the GEM model it is due to the lower resolution of the variable-resolution part of its domain.

For a limited-area data-assimilation system, the open lateral boundary conditions complicate matters (e.g. Gustaffson, 1990; Daley, 1991). They generally overconstrain the analyses near the boundaries, which can lead to errors at the scale of the limited area, and they also make it more difficult to obtain realistically-balanced analyses. Gustaffson (1990) has shown that forecast accuracy can be significantly degraded, even over the center of the forecast area, when the lateral boundary conditions used in the assimilation cycle are insufficiently accurate. This can occur due to inaccuracies in the forecasts of the driving model initiated from analyses valid 6h or 12h prior to the current analysis time. It is possible in principle to allow recently-observed data (e.g. at the current analysis time), if available in sufficient quantity and of sufficient accuracy, to correct a trial field in the vicinity of the lateral boundaries at the current analysis time. This strategy can however only be expected to be partially successful, since it leads to further discrepancies between the internally-determined flow over the limited-area and the cross-boundary flow as incorrectly specified (by hypothesis) by the driving model. It has

been found in practice at the UKMO that the mesoscale model has to be run after the larger-scale driving model, so that up-to-date data is used in the provision of the synoptic driving fields. The effect of this is exactly the same as using the single-model strategy proposed herein.

For a continuous global data-assimilation system that uses a variable-resolution model, such as the GEM one, the variable resolution can potentially cause two problems. First, an analysis climate drift is possible. Since it is strongly constrained by the lateral boundary conditions such a problem is less likely to occur in a limited-area data assimilation system, provided the limited area is not too large and the large-scale driving system does not have a climate drift. Second, even if there is no climate drift, accuracy may be degraded over the high-resolution area due to the advection of poorly-represented information from low-resolution parts of the domain. Whether such problems occur depends on the extent to which resolution is poor outside the high-resolution subdomain, and on whether the data density and quality is sufficient to give accurate analyses for those parts of the domain that influence the accuracy of the ensuing forecast over the area of interest.

The above considerations motivate the development of a regional data-assimilation spin-up cycle (e.g. Di Mego et al., 1992; Chouinard et al., 1994; Rogers et al., 1996). Spin-up data assimilation systems provide well-balanced analyses and reduce the time it takes from forecast initiation to achieve realistic precipitation rates. A typical period for a spinup cycle is 12 h. This is a good compromise between being long enough to address the precipitation spin-up problem, but short enough that poorly-resolved information does not propagate too far inwards and thereby deteriorate the analysis and subsequent forecast. Note that high resolution over data-sparse regions such as the Pacific is not guaranteed to lead to better analyses, since data sparsity is probably the factor that most limits the accuracy of analyses there. This means that the resolution over the eastern Pacific of the operational regionally-configured GEM model is probably quite sufficient for the purposes of a 12-h spin-up data-assimilation cycle. This would probably also be the case if the mesh were to be configured for short-range forecasting for Western Europe.

A possible advantage of a variable-resolution assimilation system compared to a limited-area one is that recently-observed data is more likely to improve the quality of the analysis in the vicinity of the internal boundary between the uniform-resolution subdomain and the variable-resolution part of the mesh. The data is assimilated naturally in this region without doing anything special. The analysis can then be expected to be in realistic balance, and the ensuing forecast should also remain in good balance throughout the forecast period since there cannot be any inconsistency between it and some independently, and possibly wrongly, determined boundary conditions provided by a driving model. Also, recent data *outside* a uniform-resolution subdomain can improve the analysis over the uniform-resolution subdomain, since the length scale of horizontal correlation functions can be sufficiently large that a piece of data *outside* the uniform-resolution sub-domain can influence the analysis *within* it. The current analysis of most if not all limited-area assimilation systems cannot benefit from such data because it is not used.

The GEM model and a 3-d variational (3dvar) data assimilation system (Gauthier et al., 1996), driven by the CMC's spectral model, were developed concurrently. This affected both the development of a GEM-driven data-assimilation system and the staged operational implementation of the GEM model at the CMC (see Côté et

al., 1998a, for further details). For practical reasons the GEM model was initially operationally implemented for regional forecasting without a spin-up cycle in the belief that the GEM model's performance justified this, pending the availability of a 3dvar-based spinup system. Seven month's later, a GEM-driven 3dvar regional spin-up and forecast cycle was operationally implemented . The spin-up cycle uses the incremental approach (Courtier et al., 1994) where innovations are computed in observation space with respect to the background state at the model's full resolution, whereas global analysis increments are calculated at lower resolution. This is described in detail by its developers in two recent publications (Gauthier et al. 1999, Laroche et al. 1999). Tests conducted with thirty-three cases drawn from the four seasons, plus the results from the two-month pre-implementation period, show that both the analyses and the forecasts improve on average when using this spin-up cycle, and precipitation spin-up time is considerably reduced. Priorities for further development of this system include: producing the analysis increments directly on model surfaces; improving the specification of the background error statistics; and making better use of both conventional and remotely-sensed data .

Some of the more promising 4-d data-assimilation techniques require the tangent linear model (TLM), and its adjoint, of the underlying atmospheric forecast model to be developed. The TLM and its adjoint for the adiabatic hydrostatic primitive equation version of the GEM model have been developed by the authors' colleagues, Saroja Polavarapu and Monique Tanguay. These are currently being used by them for sensitivity studies, and work is underway to build on both this work and the existing 3dvar system to develop a 4dvar system using the GEM model.

6. MODEL FORMULATION

6.1 Governing equations

The non-hydrostatic Euler equations version of the model is currently undergoing validation. Currently both the short-range regional and medium-range operational configurations of the GEM model employ the forced hydrostatic primitive equations:

$$\frac{d\mathbf{V}^H}{dt} + R_d T_v \nabla \ln p + \nabla\phi + f\left(\mathbf{k}\times\mathbf{V}^H\right) = \mathbf{F}^H, \tag{6.1}$$

$$\frac{d}{dt}\ln\left|\frac{\partial p}{\partial\eta}\right| + \nabla\cdot\mathbf{V}^H + \frac{\partial\dot{\eta}}{\partial\eta} = 0, \tag{6.2}$$

$$\frac{d}{dt}\left[\ln\left(\frac{T_v}{T^*}\right) - \kappa\ln\left(\frac{p}{p^*}\right)\right] - \kappa\dot{\eta}\frac{d}{d\eta}\left(\ln p^*\right) = F^{T_v}, \tag{6.3}$$

$$\frac{dq_v}{dt} = F^{q_v} \tag{6.4}$$

$$\frac{\partial\phi}{\partial\eta} = -R_d T_v \frac{\partial \ln p}{\partial\eta}, \tag{6.5}$$

where

$$p = \rho R_d T_v, \tag{6.6}$$

and

$$\frac{d}{dt} = \frac{\partial}{\partial t} + \mathbf{V}^H\cdot\nabla + \dot{\eta}\frac{\partial}{\partial\eta}, \tag{6.7}$$

is the substantive derivative following the fluid. Here, $\mathbf{V}^H$ is horizontal velocity, $\phi \equiv gz$ is the geopotential height, ρ is density, T_v is virtual temperature, $\kappa = R_d / c_{pd}$, R_d is the gas constant for dry air, c_{pd} is the specific heat of dry air at constant pressure, q_v is specific humidity of water vapour, f is the Coriolis parameter, $\mathbf{k}$ is a unit vector in the vertical, g is the vertical acceleration due to gravity, p^* and T^* are basic state pressure and temperature respectively, and $\mathbf{F}^H$, F^{T_v}, and F^{q_v} are parameterized forcings (see below). Eqs. (6.1)-(6.4) are respectively the horizontal momentum, continuity, thermodynamic, and moisture equations, and (6.6) is the equation of state, taken here to be the ideal gas law. The prognostic vertical momentum equation of the fully-compressible Euler equations has been reduced here to the diagnostic hydrostatic equation (6.5).

6.2 Boundary conditions

The boundary conditions are periodicity in the horizontal; and no motion across the top and bottom of the atmosphere, where the top is at constant pressure p_T. Thus

$$\dot{\eta} \equiv \frac{d\eta}{dt} = 0 \text{ at } \eta = 0,1. \tag{6.8}$$

6.3 Transport equations

To the above set of governing equations are appended transport equations for various ancillary quantities. These are taken in the form

$$\frac{d\Psi_i}{dt} = F^{\Psi_i}, \tag{6.9}$$

where Ψ_i is the i'th atmospheric tracer and F^{Ψ_i} is its parameterized forcing. Example atmospheric tracers include cloud liquid water and chemical species such as ozone, hydrocarbons and aerosols. The advective form (6.9) of the transport equations is equivalent to the flux form

$$\frac{\partial}{\partial t}(\rho\Psi_i) + \nabla_3 \cdot (\rho\Psi_i \mathbf{V}_3) = \rho F^{\Psi_i}, \tag{6.10}$$

where ∇_3 and $\mathbf{V}_3$ are respectively the three-dimensional gradient operator and velocity vector.

6.4 Temporal discretization

Eqs. (6.1)-(6.5) are first integrated in the absence of forcing, and the parameterized forcing terms appearing on the right-hand sides of (6.1)-(6.4) are then computed and added using the usual fractional-step time method (Yanenko, 1971).

The time discretization used to integrate the frictionless adiabatic equations of the first step is implicit/ semi-Lagrangian. Consider a prognostic equation of the form

$$\frac{dF}{dt} + G = 0, \tag{6.11}$$

where F represents one of the prognostic quantities $\{ \mathbf{V}^H,\ \ln|\partial p/\partial\eta|,\ \ln(T_v/T^*) - \kappa \ln(p/p^*) \}$, and G represents the remaining terms, some of which are nonlinear. Such an equation is approximated by time differences and weighted averages along a trajectory determined by an approximate solution to

$$\frac{d\mathbf{x}_3}{dt} = \mathbf{V}_3(\mathbf{x}_3, t), \tag{6.12}$$

where $\mathbf{x}_3$ and $\mathbf{V}_3$ are the three-dimensional position and velocity vectors respectively. Thus

$$\frac{\left(F^n - F^{n-1}\right)}{\Delta t} + \left[\left(\frac{1}{2}+\varepsilon\right)G^n + \left(\frac{1}{2}-\varepsilon\right)G^{n-1}\right] = 0, \tag{6.13}$$

where $\psi^n = \psi(\mathbf{x}_3, t)$, $\psi^{n-1} = \psi[\mathbf{x}_3(t-\Delta t), t-\Delta t]$, $\psi = \{F, G\}$, $t = n\Delta t$.

Note that this scheme is decentered along the trajectory as in Rivest et al. (1994), to avoid the spurious resonant response arising from a centered approximation in the presence of orography. The off-centering parameter ε is currently set to 0.1 for both the short- and the medium-range operational configurations. Cubic interpolation is used everywhere for upstream evaluations (cf. 6.13) except for the trajectory computations (cf. 6.12), where linear interpolation is used with no visible degradation in the results.

Grouping terms at the new time on the left-hand side and known quantities on the right-hand side, (6.13) may be rewritten as

$$\left[F + \left(\frac{1}{2}+\varepsilon\right)\Delta t G\right]^n = \left[F - \left(\frac{1}{2}-\varepsilon\right)\Delta t G\right]^{n-1}. \tag{6.14}$$

This yields a set of coupled nonlinear equations for the unknown quantities at the meshpoints of a regular grid at the new time t, the efficient solution of which is briefly discussed below. An implicit time treatment, such as that adopted here, of the nonlinear terms has the useful property of being inherently computationally more stable than an explicit one (see e.g. the Gravel et al., 1993 , analysis). To ensure the stability of the aforementioned implicit treatment, the trajectory equation (6.12) is also solved in a time-implicit manner. This is done by first using the time-extrapolated 3-d wind at time $t - \Delta t/2$ to obtain an estimate of the displacements (cf. 6.12) and solution. These are then corrected by using the time-interpolated wind at $t - \Delta t/2$ to obtain the final displacements and solution.

6.5 Spatial discretization

A variable-resolution cell-integrated finite-element discretization on an Arakawa C grid is used in the horizontal with a placement of variables as shown in Fig. 5 of Côté et al. (1998a). For uniform resolution it reduces to the usual staggered finite-difference formulation in spherical geometry (e.g. Bates et al., 1993; Cullen et al., 1997). The Arakawa C placement of variables is considered to be the best one when the meshlength is less than the Rossby radius of deformation (Arakawa and Lamb, 1977; Cullen et al., 1997), making it suitable for mesoscale applications.

Due to the staggering of variables, there is a certain arbitrariness with a C grid in how the upstream interpolations of a semi-Lagrangian scheme are made. In the GEM model these interpolations are performed using the grid associated with the placement of scalar quantities. The right-hand sides $R_U\left[\mathbf{x}_3^U(t)\right]$ and $R_V\left[\mathbf{x}_3^V(t)\right]$ of the horizontal momentum equations are first interpolated to the scalar grid using 1-d cubic Lagrange interpolation, where $\mathbf{x}_3^U(t)$ and $\mathbf{x}_3^V(t)$ respectively are the arrival points of the U and V grids. This is simply a local four-point weighted averaging along each of the two coordinate directions, and the result is denoted by $R_{\mathrm{V}}^s \equiv \left(R_U^s, R_V^s\right)$, where superscript " s " refers to the scalar grid. $R_{\mathrm{V}}^s\left[\mathbf{x}_3^s(t)\right]$ is then interpolated to the upwind position $\mathbf{x}_3^s(t-\Delta t)$, where $\mathbf{x}_3^s(t)$ is an arrival point of the scalar grid. Next, a metric correction

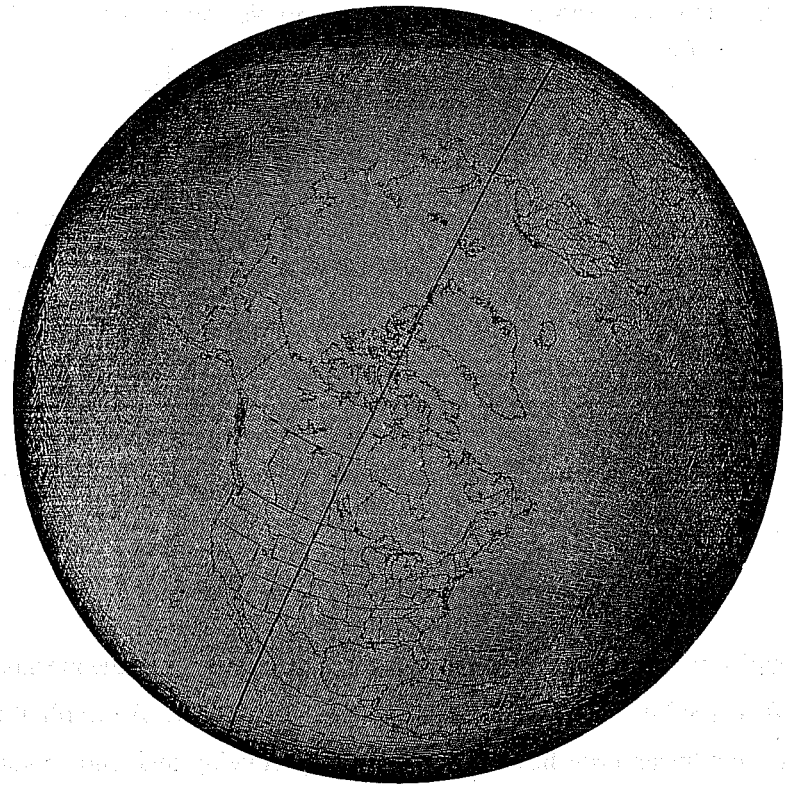

Fig. 5(a) The uniform 0.36° resolution 1000 x 500 mesh used for Expt . B.

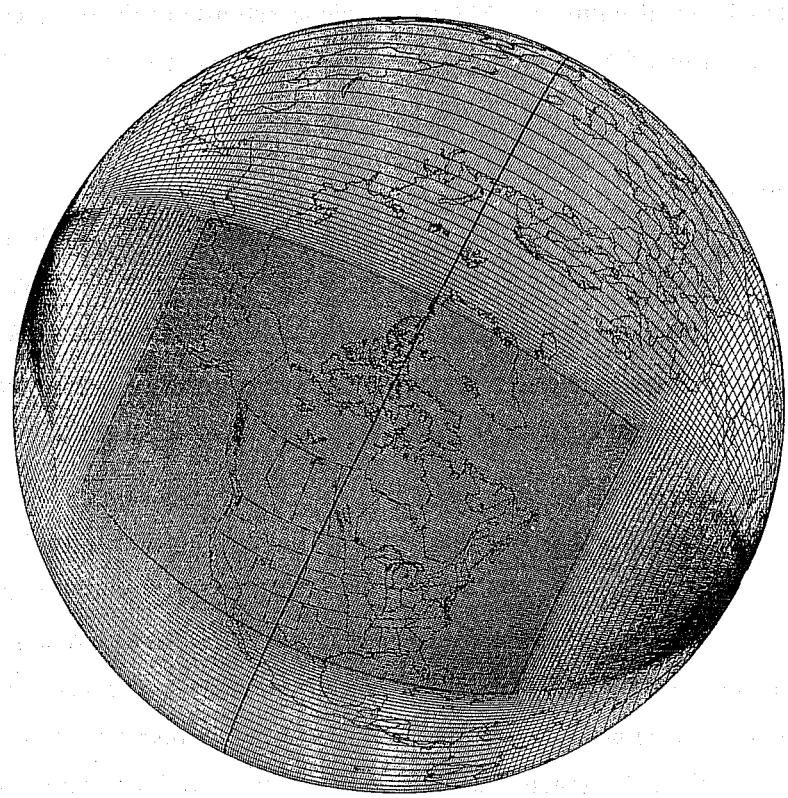

Fig. 5(b) A variable-resolution 240 x 268 mesh having a 59.04° x 76.68° window of uniform 0.36° resolution, centred on (100°W, 58°N), and used for Expt C.

term δ_V^s is computed to ensure that horizontal displacements are spherically constrained (Côté, 1988), and increments are defined on the scalar grid by

$$\left(\Delta R_U^s, \Delta R_V^s\right) \equiv \left\{R_V^s\left[\mathbf{x}_3^s(t-\Delta t)\right] + \delta_V^s\right\} - R_V^s\left[\mathbf{x}_3^s(t)\right]. \tag{6.15}$$

The increments ΔR_U^s and ΔR_V^s are then respectively interpolated back to the U and V grids using 1-d cubic Lagrange interpolation and denoted by ΔR_U^U and ΔR_V^V, where the superscripts refer to the corresponding grids. This is followed by corrections of the original fields R_U and R_V. Thus

$$\left(R_U, R_V\right)\Big|_{upstream} \equiv \left\{R_U\left[\mathbf{x}_3^U(t-\Delta t)\right], R_V\left[\mathbf{x}_3^V(t-\Delta t)\right]\right\} = \left\{R_U\left[\mathbf{x}_3^U(t)\right], R_V\left[\mathbf{x}_3^V(t)\right]\right\} + \left(\Delta R_U^s, \Delta R_V^s\right), \tag{6.16}$$

where $\mathbf{x}_3^U(t-\Delta t)$ and $\mathbf{x}_3^V(t-\Delta t)$ respectively denote the upstream points associated with the arrival points $\mathbf{x}_3^U(t)$ and $\mathbf{x}_3^V(t)$.

The vertical discretization is modeled after that of Tanguay et al. (1989).

6.6 Solving the coupled nonlinear set of discretized equations

After spatial discretization the coupled set of nonlinear equations still has the form of (6.14). Terms on the right-hand side, which involve upstream interpolation, are evaluated once and for all. The coupled set is rewritten as a linear one (where the coefficients depend on the basic state) plus a perturbation which is placed on the right-hand side and which is relatively cheap to evaluate. The nonlinear set is then solved iteratively using the linear terms as a kernel (the linear set can be algebraically reduced to the solution of an equivalent 3-d elliptic-boundary-value problem), and the nonlinear terms on the right-hand side are re-evaluated at each iteration using the most-recent values. The Generalized Conjugate Gradient Method of Concus et al. (1976) is used as a convergence accelerator. Two iterations have been found sufficient for practical convergence.

6.7 Physical parameterization

To close the problem, the source, sink and redistribution terms of the right-hand sides of (6.1)-(6.4) must be specified or parameterized. These forcings are associated with both unrepresented and sub-grid-scale phenomena. The GEM model has therefore been interfaced with the unified RPN (Recherche en prévision numérique) physics package. A recent description of the current operational parameterizations contained within the package may be found in Mailhot et al. (1997).

The choice of parameterization depends upon the space and time scales of the application and the resolution of the forecast or simulation (e.g. Bougeault 1997). For example, a detailed and expensive radiation calculation is an essential ingredient for climate-scale simulations, but much less so for short- and medium- range weather forecasting. Also the appropriate treatment of convection is very different (e.g. Weisman et al., 1997) between a large-scale application where it is parameterized, and a meso-γ-scale application where it may be parameterized very differently or even represented explicitly. It is also useful to experiment with different parameterizations of a given process. For example, three different land-surface parameterization schemes are available at RPN: the operational force-restore one, the CLASS scheme (Verseghy, 1991, 1993) of the AES's Climate Branch, and the ISBA scheme (Bélair et al., 1997) of Météo France.

In the context of a variable-resolution model, there can be a considerable disparity between the resolution of the uniform-resolution sub-domain and that geographically far away from it. A frequently-asked question is then: what does one do in this context regarding parameterization? In our view parameterizations should be chosen to be appropriate to the resolution of the high- and uniform- resolution subdomain. Provided that they do not behave pathologically at low resolution (in which case they could be simply switched off there, making the model somewhat more efficient), then there is simply insufficient time during the period of integration for their errors to reach the area of interest (i.e. a sub-area of the area of uniform resolution) and contaminate it. Parameterizations should be formulated, to the extent possible, such that a measure of the model's local resolution is a parameter used to determine local aggregations and local threshold values of trigger functions, thereby extending their validity as a function of resolution. This would reduce the need for retuning parameters each time the resolution is changed within the validity regime associated with the underlying parameterization hypotheses.

6.8 **Digital filter diabatic finalization**

Digital filtering is proving to be a good method for the diabatic initialization of weather forecasts models (e.g. Lynch and Huang, 1994). For the model described herein, the digital filtering diabatic finalization technique described in Fillion et al. (1995) is used to filter out high-frequency oscillations having periods smaller than 6 h. A 6-h forward integration of the complete model, including all the diabatic forcing terms, generates a time series of model states. These are filtered as this 6-h integration progresses in time leading to a time-filtered state that is valid 3h into the integration. The model is then integrated forward in time in the usual way by restarting the integration at 3h using this time-filtered state.

7. ASSESSING THE STRATEGY FOR CONTINENTAL-SCALE REGIONS

7.1 **Methodology**

A preliminary assessment of the global variable-mesh strategy for continental-scale regions was made in Côté et al. (1997) by comparing uniform- and variable-resolution 48-h integrations started from the same initial data, using the methodology introduced in Côté et al. (1993) for the validation of a shallow-water prototype. The same validation methodology is adopted here. However the GEM model now includes topography and all the physical parameterizations (Mailhot et al., 1997) used operationally for regional forecasting, and the experiments are performed at substantially-higher (0.36°) resolution. Ideally they should be run at the 0.33° resolution of the uniform-resolution window of the mesh displayed in Fig. 1. Unfortunately computer memory limitations at the time the experiment was run did not permit uniform-resolution control forecasts at quite such a high resolution.

Three 48-h integrations are made starting from the same initial data, the CMC 16-level isobaric analysis valid at 12 UTC 14 Nov 95. The strong flow over the eastern Pacific, upstream of N. America, is of particular interest here. A digital filtering technique based on that described in Fillion et al. (1995) was employed in all experiments to put the fields in dynamic balance, and all integrations were performed with: the 28 vertical levels shown schematically in Fig. 1 of Côté et al. (1998b); a timestep of 22.5 mins; and a Laplacian diffusion with a coefficient of $2 \times 10^4 \, m^2 s^{-1}$. The three experimental configurations are summarized in Table 1. The purpose of

the two *uniform*-resolution experiments is to validate a uniform-resolution ground truth (Expt. B) against which the *variable*-resolution forecast of Expt. C can be compared and evaluated. Both uniform-resolution experiments were performed at 0.36° resolution (in both longitude and latitude), using a mesh with the poles of the coordinate system either coincident with respect to the geographical ones (Expt. A), or rotated (Expt. B) as in Fig. 5a.

Expt.	Rotated Coordinate System?	Mesh Dimensions	Uniform/ Variable	Resolution
A	No	1000 x 500	Uniform	0.36° everywhere
B	Yes, centred on (100°W, 58°N)	1000 x 500	Uniform	0.36° everywhere
C	Yes, centred on (100°W, 58°N)	240 x 268	Variable	0.36° on 59.04° x 76.68° window

Table 1: Experimental configurations.

The variable-resolution Expt. C was performed on the mesh depicted in Fig. 5b, where the poles of the coordinate system are rotated with respect to the geographical ones. Its purpose is to demonstrate the thesis that the variable-resolution forecast over the 0.36° uniform-resolution continental window well reproduces, but at a fraction of the cost, that obtained using 0.36° uniform resolution everywhere. The resolution of the mesh is uniform (0.36°) over a 59.04° x 76.68° window centered on a point of the equator of a rotated coordinate system located at 58°N, 100°W in geographical coordinates. Uniform resolution again refers to uniform spacing in latitude and longitude: however the meshpoints of the window are also almost uniformly spaced over the sphere with a meshlength that varies between approximately 31 and 40 km. Outside the window, the resolution degrades smoothly away in each direction with each successive meshlength being approximately 10% larger than its predecessor. The gradual transition from fine to coarse resolution allows an adequate representation of the flow features in the vicinity of the uniform window that are subsequently advected over the domain of interest during the course of the short-term integration. Too large an expansion factor – 25% for example – would lead to larger forecast errors over the area of interest. The cost of the uniform-resolution experiments is about seven times that of the variable-resolution experiment, a little less than the ratio of the number of grid points.

7.2 **Uniform-resolution experiments**

The 500-hPa height and mean-sea-level pressure (mslp) fields of the initial analysis used for the experiments are shown in Fig. 4 of Côté et al. (1998b). The global rms forecast differences (computed after interpolating the forecast of Expt. A to the rotated mesh of Expt. B) of the resulting 2-day forecasts of these fields for Expts. A and B (i.e. using uniform 0.36° resolution on the unrotated and rotated meshes) are 4.44 m and 0.58 hPa respectively. This shows that the effect of rotating the mesh by 83.37° along a meridian while keeping its resolution uniform is acceptably small. The 2-day forecast for Expt. B (i.e. uniform resolution everywhere in the rotated coordinate system) is shown in Fig. 6.

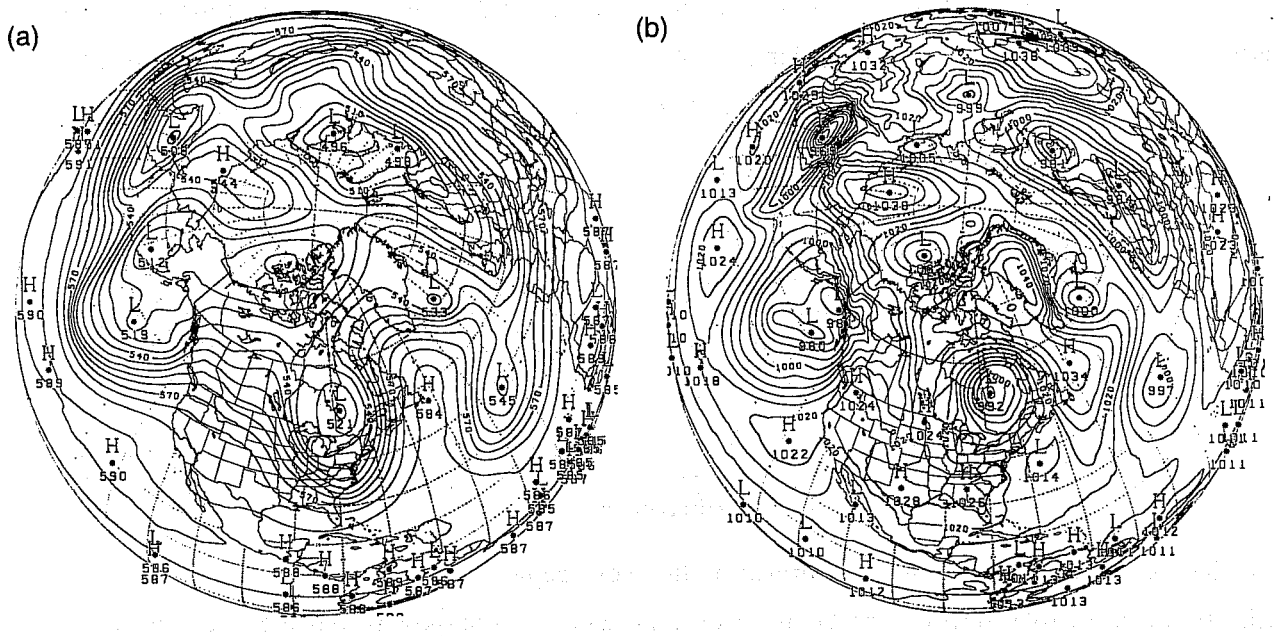

Fig. 6 48 h forecast for Expt. B, displayed on an orthographic projection:
(a) geopotential height (dam) at 500 hPa; contour interval is 6 dam.
(b) msl pressure (hPa); contour interval is 4 hPa.

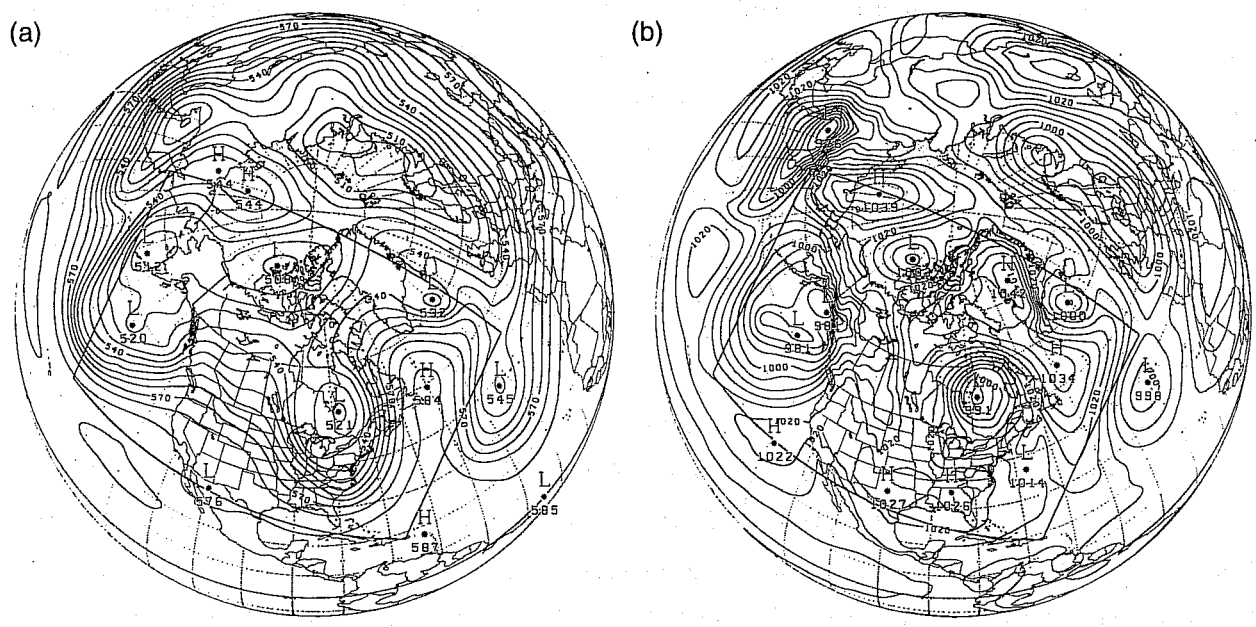

Fig. 7 (a) Same as in Fig. 6a, but for Expt. C.
(b) Same as in Fig. 6b, but for Expt. C.

7.3 Variable-resolution experiment

Experiment B is considered to be the ground truth for the purposes of validating the 48h forecast of the variable-resolution integration (Expt. C): note that the meshes of both integrations are identical over the uniform-resolution window of Fig. 5b. The 2-day variable-resolution forecast is shown in Fig. 7 and may be compared to that of the control (Fig. 6). The two forecasts (Expts. B vs. C) are quite close over the uniform-resolution area of interest (defined by the curvilinear rectangle of Fig. 7a). This confirms the thesis that the variable-resolution forecast over the 0.36° uniform-resolution continental window well reproduces, but at a fraction of the cost, that obtained using 0.36° uniform resolution everywhere. However they are significantly different over areas of low resolution, as indeed they should be. The differences (see Fig. 8) between the forecasts of Expts. B and C increase as a function of distance from the boundary of the uniform-resolution window, consistent with theory. Quantifying this, the global rms differences between the forecasts of Expts. B and C are 42.3 m and 3.85 hPa for the 500 hPa height and mslp fields respectively, whereas they are only 5.24 m and 0.48 hPa over the curvilinear rectangle, where the meshpoints of the two grids are coincident. These latter differences are of the same order as those between Expts. A and B computed over the same curvilinear rectangle (3.85 m and 0.66 hPa respectively), which both use the same uniform-resolution meshes but rotated with respect to one another.

8. SUMMARY

To meet the needs of operational weather forecasting and research, as well as those of air-quality and climate modelling, a unified strategy is proposed that is based on the use of a global variable-resolution model, run with different configurations. Broadly speaking, these are:

- a uniform-resolution 'global-scale' configuration, for large-scale problems such as medium- and long-range weather forecasting, climate change modelling, and the long-range transport of pollutants;
- a variable-resolution 'synoptic-scale' configuration for regional-scale problems such as more detailed forecasts to 2 days, and regional air-quality and climate modelling; and
- variable-resolution meso-β and meso-γ configurations for yet-more-detailed forecasts and simulations at correspondingly-shorter time periods.

This approach offers economies in both operational and research environments, since there is only one model to maintain, develop and optimize, instead of the usual two or more. It also provides a viable and conceptually-simple solution to the nesting problem for regional forecasting: the planetary-scale waves are adequately resolved around a high-resolution subdomain (which resolves the smaller-scale disturbances); there are no artificial lateral boundaries; and there is no abrupt change of resolution across an internal boundary since the resolution varies smoothly away from the area of interest.

Ingredients of this strategy include:

- an implicit time treatment of the non-advective terms responsible for the fastest-moving acoustic and gravitational oscillations;
- a semi-Lagrangian treatment of advection to overcome the stability limitations encountered in Eulerian schemes due to the convergence of the meridians and to strong jet streams;
- a cell-integrated finite-element spatial discretization to provide a robust way of achieving variable resolution;

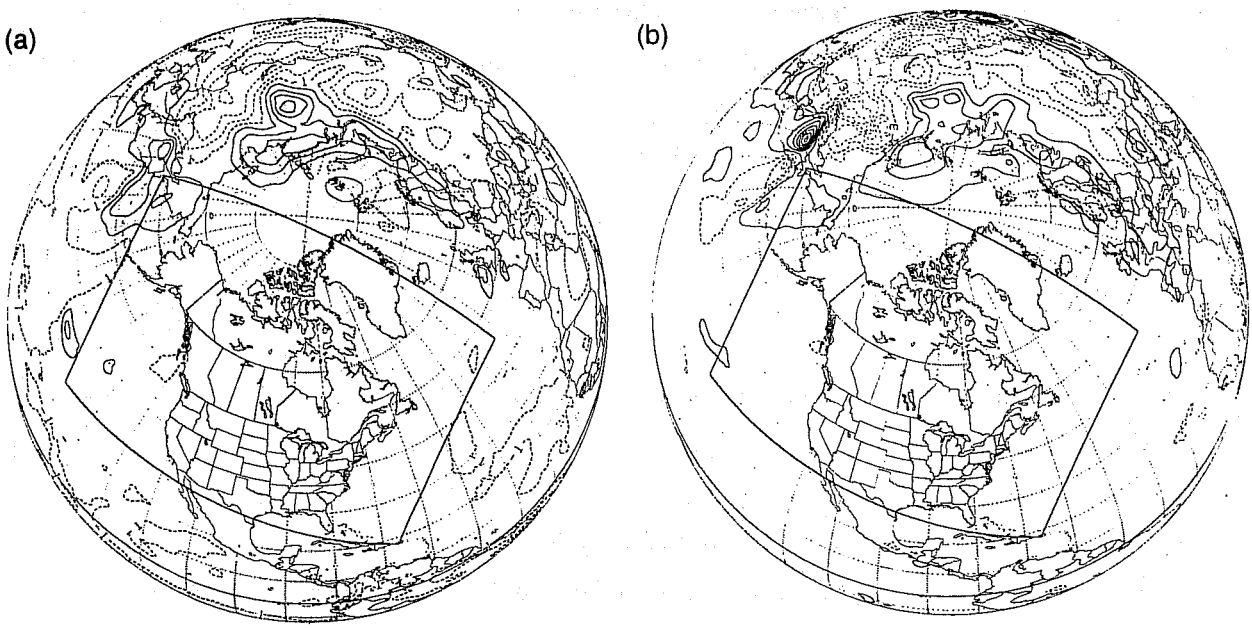

Fig. 8 Difference between 48-h forecasts of Expts. B and C on an orthographic projection for:
(a) 500 hPa geopotential height; contours are ±10, ±30, ±50, ... m.
(b) msl pressure; contours are ±1, ±3, ±5, ... hPa.

- an arbitrary-rotated latitude-longitude mesh to focus resolution on any part of the globe;
- an embedded advection-diffusion module to transport a family of chemical species for air-quality and environmental-emergency-response applications;
- a 3-d variational data assimilation system (to be described in detail elsewhere); and
- a tangent linear model and its adjoint to facilitate the development of future 4d data assimilation systems.

For regional forecasting at the continental scale, the above-described controlled set of experiments show that differences between the 48-h forecasts for the 500 hPa geopotential height and mean-sea-level pressure fields obtained from a uniform horizontal resolution integration, and those obtained from a variable-mesh one with equivalent resolution over a N. American window, are acceptably small.

More extensive results for regional and other applications over a broad range of scales may be found in Côté et al. (1998b). These include: further results for regional forecasting; a comparison of medium-range integrations of the GEM model with those of a spectral model; and a meso-γ-scale simulation.

On 24 Feb 1997 a 0.33° *variable*-resolution configuration of the GEM model with 28 levels replaced CMC's then-operational Regional Finite Element model, to provide 48-h weather forecasts over N. America twice daily. Since 24 Sept 1997, the initial conditions are obtaind from a GEM-driven 3dvar regional data-ssimilation spin-up cycle. The horizontal resolution of this regional data-assimilation and forecast cycle was upgraded to 0.22° resolution over N. America on 15 Sept 1998. A month later, on 14 Oct 1998, a 0.9° *uniform*-resolution configuration of the GEM-driven 3dvar data-assimilation and medium-range forecasting system replaced CMC's then-operational spectral model. This completed the unification of CMC's short- and medium-range assimilation and forecasting cycles.

ACKNOWLEDGEMENTS

The authors gratefully acknowledge the continuous support by the managers - Hubert Allard, Michel Béland, Peter Chen, Jean-Guy Desmarais, Pierre Dubreuil, Louis Lefaivre, Réal Sarrazin, Angèle Simard and David Steenbergen - of the AES during the development phase of the project described herein.

Many of the authors' colleagues made very valuable technical contributions to the development of the GEM model. Particular thanks are due to James Caveen, Yves Chartier, Gabriel Lemay, Judy St. James, Joseph-Pierre Toviessi and Michel Valin. Thanks are also due to Pierre Gauthier, Stéphane Laroche, Josée Morneau, Saroja Polavarapu, Judy St. James and Monique Tanguay for their work, briefly summarized here and described in detail by them elsewhere, on the complementary data assimilation aspects of the project.

For their technical support and their contribution to the evaluation of the new model's performance, the authors are also grateful to: Michel Baltazar, Bernard Bilodeau, Normand Brunet, Gérard Croteau, Louise Faust, Michel Grenier, Patrick Hertel, Richard Hogue, Doug Bender, André Plante, Richard Verret, and CMC's operational meteorologists.

REFERENCES

Anthes, R.A., 1983: Regional models of the atmosphere in middle latitudes. *Mon. Wea. Rev.*, **111**, 1306-1335.

Arakawa, A., and V.R. Lamb, 1977: Computational design of the basic dynamical processes of the UCLA general circulation model. *Methods in Computational Physics*, **17**, Academic Press, 174-265.

Arakawa, A., 1984: Boundary conditions in limited-area models. *Proceedings of the Workshop on Limited-Area Numerical Weather Prediction Models for Computers of Limited Power.* Short- and Medium- Range Weather Prediction Research Publication Series, No. 13 (WMO/TD No. 19), World Meteorological Organisation, Geneva, 403-436.

Bates, J.R., S. Moorthi, and R.W. Higgins, 1993: A global multilevel atmospheric model using a vector semi-Lagrangian finite-difference scheme. Part I: adiabatic formulation. *Mon. Wea. Rev.*, **121**, 244-263.

Bélair, S., P. Lacarrère, J. Noilhan, V. Masson, and J. Stein, 1997: High-resolution simulation of surface and turbulent fluxes during HAPEX-MOBILHY. *Mon. Wea. Rev.*, accepted

Bermejo, R., and A. Staniforth, 1992: The conversion of semi-Lagrangian advection schemes to quasi-monotone schemes. *Mon. Wea. Rev.*, **120**, 2622-2632.

Bougeault, P., 1997: Physical parameterization for limited area models: some current problems and issues. *Meteor. Atmos. Phys.*, **63**, 71-88.

Bubnova, R., G. Hello, P. Bénard, and J.-F.Geleyn, 1995: Integration of the fully elastic equations cast in hydrostatic pressure terrain-following coordinate in the framework of the ARPEGE/ Aladin NWP system. *Mon. Wea. Rev.*, **129**, 515-535.

Caian, M., and J.-F. Geleyn, 1997: Some limits to the variable mesh solution and comparison with the nested LAM one. *Q. J. Roy. Met. Soc.*, **123**, 743-766.

Chouinard, C., J. Mailhot, H.L. Mitchell, A. Staniforth, and R. Hogue, 1994: The Canadian regional data assimilation system: operational and research applications. *Mon. Wea. Rev.*, **122**, 1306-1325.

Concus, P., G.H. Golub, and D.P. O'Leary, 1976. A generalized conjugate gradient method for the numerical solution of partial differential equations. *Sparse Matrix Computations* (eds. R. Bunch and D.J. Rose), Academic Press, New York, 309-322.

Côté, J., 1998: A Lagrange multiplier approach for the metric terms of semi-Lagrangian models on the sphere. *Q. J. Roy. Meteor. Soc.*, **114**, 1347-1352.

Côté, J., M. Roch, A. Staniforth, and L. Fillion, 1993: A variable-resolution semi-Lagrangian finite-element global model of the shallow-water equations. *Mon. Wea. Rev.*, **121**, 231-243.

Côté, J., S. Gravel, A. Méthot, A. Patoine, M. Roch, and A. Staniforth, 1997: Preliminary results from a dry global variable-resolution primitive equations model. The André J. Robert Memorial Volume (companion volume to *Atmosphere-Ocean*), Eds. C. Lin, R. Laprise, H. Ritchie, 245-259, Canadian Meteorological & Oceanographic Society, Ottawa, Canada.

Côté, J., S. Gravel, A. Méthot, A. Patoine, M. Roch, and A. Staniforth, 1998a: The operational CMC-MRB Global Environmental Multiscale (GEM) model: Part I. Design considerations and formulation. *Mon. Wea. Rev.*, **126**, 1373-1395.

Côté, J., J.-G. Desmarais, S. Gravel, A. Méthot, A. Patoine, M. Roch, and A. Staniforth, 1998b: The operational CMC-MRB Global Environmental Multiscale (GEM) model: Part II. Results. *Mon. Wea. Rev.*, **126**, 1397-1418.

Courtier, P., and J.-F. Geleyn, 1988: A global numerical weather prediction model with variable resolution: application to the shallow-water equations. *Q. J. Roy. Met. Soc.*, **114**, 1321-1346.

Courtier, P., C. Freydiet, J.-F. Geleyn, F. Rabier, and M. Rochas, 1991: The Arpege project at Météo France. *Proc. Numerical Methods in Atmospheric Models*, European Centre for Medium-range Weather Forecasts, Shinfield Park, Reading, UK, 193-231.

Courtier, P., J.-N. Thépaut, and A. Hollingsworth, 1994: A strategy for operational implementation of 4D-Var, using an incremental approach. *Q. J. Roy. Meteor. Soc.*, **120**, 1367-1388.

Cullen, M.J.P., 1993: The unified forecast/ climate model. *Meteorological Magazine*, **122**, 81-94.

Cullen, M.J.P., T. Davies, M.H. Mawson, J.A. James, and S.C. Coulter, 1997: An overview of numerical methods for the next generation UK NWP and climate model. The André J. Robert Memorial Volume (companion volume to *Atmosphere-Ocean*), Eds. C. Lin, R. Laprise, H. Ritchie, 425-444, Canadian Meteorological & Oceanographic Society, Ottawa, Canada.

Daley, R.W., 1991: *Atmospheric Data Analysis*. Cambridge Atmospheric and Space Science Series, vol. 2, Cambridge University Press, 457 pp.

DiMego, G.J., K.E. Mitchell, R.A. Petersen, J.E. Hoke, J.P. Gerrity, J.C. Tuccilo, R.L. Wobus, and H.H. Juang, 1992: Changes to NMC's regional analysis and forecast system. *Wea. Forecasting*, **7**, 185-198.

Errico, R., and D. Baumhefner, 1987: Predictability experiments using a high-resolution limited-area model. *Mon. Wea. Rev.*, **115**, 488-504.

Errico, R.M., T. Vukicevic, and K. Raeder, 1993: Comparison of initial and lateral boundary condition sensitivity for a limited-area model. *Tellus*, **45A**, 539-557.

Fillion, L., H.L. Mitchell, H. Ritchie, and A. Staniforth, 1995: The impact of a digital filter finalization technique in a global data assimilation system. *Tellus*, **47A**, 304-323.

Fox-Rabinovitz, M., G. Stenchikov, M. Suarez, and L. Takacs, 1997: A finite-difference GCM dynamical core with a variable resolution stretched grid. *Mon. Wea. Rev.*, **125**, 2943-2968.

Gauthier, P., L. Fillion, P. Koclas, and C. Charette, 1999: Implementation of a 3D variational assimilation system at the Canadian Meteorological Centre. Part I: the global analysis. *Atmos.-Ocean*, **37**, to appear.

Gravel, S., and A. Staniforth, 1992: Variable resolution and robustness. *Mon. Wea. Rev.*, **120**, 2633-2640.

Gravel, S., A. Staniforth, and J. Côté, 1993: A stability analysis of a family of baroclinic semi-Lagrangian forecast models. *Mon. Wea. Rev.*, **121**, 815-826.

Gustafsson, N., 1990: Sensitivity of limited area model data assimilation to lateral boundary condition fields. *Tellus*, **42A**, 109-115.

Hardiker, V., 1997: A global numerical weather prediction model with variable resolution. *Mon. Wea. Rev.*, **125**, 59-73.

Harrison, E.J., and R.L. Elsberry, 1972: A method of incorporating nested finite grids in the solution of systems of geophysical equations. *J. Atmos. Sci.*, **29**, 1235-1245.

Held, I.M., and M.J. Suarez, 1994: A proposal for the intercomparison of the dry dynamical cores of atmospheric general circulation models. *Bull. Amer. Meteor. Soc.*, **75**, 1825-1830.

Kalnay de Rivas, E., 1972: On the use of nonuniform grids in finite-difference equations. *J. Comput. Phys.*, **10**, 202-210.

Kasahara, A., 1974: Various vertical coordinate systems used for numerical weather prediction. *Mon. Wea. Rev.*, **102**, 509-522.

Kurihara, Y., and R. E. Tuleya, 1974: Structure of a tropical cyclone developed in a three-dimensional numerical simulation model. *J. Atmos. Sci.*, **31**, 893-919.

Laprise, R., 1992: The Euler equations of motion with hydrostatic pressure as independent variable. *Mon. Wea. Rev.*, **120**, 197-207.

Laroche, S., P. Gauthier, J. St. James, and J. Morneau, 1999: Implementation of a 3d variational data assimilation system at the Canadian Meteorological Centre. Part ii: the regional analysis. *Atmos.-Ocean*, submitted.

Lynch, P., and X.-Y. Huang, 1994. Diabatic initialization using recursive filters. *Tellus*, **46A**, 583-597.

Mailhot, J., R. Sarrazin, B. Bilodeau, N. Brunet, and G. Pellerin, 1997: Development of the 35-km version of the operational regional forecast system. *Atmos.-Ocean*, **35**, 1-28.

Mesinger, F., 1973: A method for construction of second-order accuracy difference schemes permitting no false two-grid-interval wave in the height field. *Tellus*, **25**, 444-458.

Oliger, J., and A. Sundström, 1978: Theoretical and practical aspects of some initial boundary value problems in fluid dynamics. *S.I.A.M. J. Appl.Math.*, **35**, 419-446.

Paegle, J., 1989: A variable resolution global model based upon Fourier and finite element representation. *Mon. Wea. Rev.*, **117**, 583-606.

Paegle, J., Q. Yang, and M. Wang, 1997: Predictability in limited area and global models. *Meteor. Atm. Phys.*, **63**, 53-69.

Phillips, N.A., 1957: A coordinate system having some special advantages for numerical forecasting. *J. Meteor.*, **14**, 184-185.

Phillips, N.A., and J. Shukla, 1973: On the strategy of combining coarse and fine grid meshes in numerical weather prediction. *J. Appl. Meteor.*, **12**, 763-770.

Priestley, A., 1993: A quasi-conservative version of the semi-Lagrangian advection scheme. *Mon. Wea. Rev.*, **121**, 621-629.

Ritchie, H., and C. Beaudoin, 1994: Approximations and sensitivity experiments with a baroclinic semi-Lagrangian spectral model. *Mon. Wea. Rev.*, **122**, 2391-2399.

Rivest, C., A. Staniforth, and A. Robert, 1994: Spurious resonant response of semi-Lagrangian discretizations to orographic forcing: Diagnosis and solution. *Mon. Wea. Rev.*, **122**, 366-376.

Robert, A., 1981: A stable numerical integration scheme for the primitive meteorological equations. *Atmos.-Ocean*, **19**, 35-46.

Robert, A., 1982: A semi-Lagrangian and semi-implicit numerical integration scheme for the primitive meteorological equations. *J. Meteor. Soc. Japan*, **60**, 319-325.

Robert, A., T.L. Yee, and H. Ritchie, 1985: A semi-Lagrangian and semi-implicit numerical integration scheme for multilevel atmospheric models. *Mon. Wea. Rev.*, **113**, 388-394.

Robert, A., and E. Yakimiw, 1986: Identification and elimination of an inflow boundary computational solution in limited area model integrations, *Atmos.-Ocean*, **24**, 369-385.

Rogers, E., T.L. Black, D.G. Deaven, G.J. DiMego, Q. Zhao, M. Baldwin, N.W. Junker, and Y. Lin, 1996: Changes to the operational "Early" Eta analysis/ forecast system at the National Centers for Environmental Prediction. *Wea. Forecasting*, **11**, 391-413.

Schmidt, F., 1977: Variable fine mesh in the spectral global models. *Beitr. Phys. Atmos.*, **50**, 211-217.

Semazzi, F.H.M., J.-H. Qian, and J.S. Scroggs, 1995: A global nonhydrostatic semi-Lagrangian atmospheric model. *Mon. Wea. Rev.*, **123**, 2534-2550.

Sharma, O.P., H. Upadhyaya, Th. Braine-Bonnaire, and R. Sadourny, 1987: Experiments on regional forecasting using a stretched coordinate general circulation model. *Short- and Medium- Range Numerical Weather Prediction,* Proceedings of WMO/ IUGG NWP Symposium, 263-271, Met. Soc. Japan, Tokyo, T. Matsuno (ed), 831 pp.

Skamarock, W.C., P.K. Smolarkiewicz, and J.B. Klemp, 1997: Preconditioned conjugate-residual solvers for Helmholtz equations in nonhydrostatic models. *Mon. Wea. Rev.*, **125**, 587-599.

Staniforth, A., 1987: Review - formulating efficient finite-element codes for flows in regular domains. *Int. J. Numer. Meth. Fluids*, **7**, 1-16.

Staniforth, A., and J. Côté, 1991: Semi-Lagrangian integration schemes for atmospheric models - a review. *Mon. Wea. Rev.*, **119**, 2206-2223.

Staniforth, A., 1997: Regional modeling: a theoretical discussion. *Meteor. Atmos. Phys.*, **63**, 15-29.

Tanguay, M., A. Simard, and A. Staniforth, 1989: A three-dimensional semi-Lagrangian scheme for the Canadian regional finite-element forecast model. *Mon. Wea. Rev.*, **117**, 1861-1871.

Tanguay, M., A. Robert, and R. Laprise, 1990: A semi-implicit semi-Lagrangian fully compressible regional forecast model. *Mon. Wea. Rev.*, **118**, 1970-1980.

Verseghy, D., 1991: CLASS - A Canadian land surface scheme for GCMs. I: Soil model. *Int J. Climatol.*, **11**, 111-113.

Verseghy, D., 1993: CLASS - A Canadian land surface scheme for GCMs. II: Vegetation model and coupled runs. *Int J. Climatol.*, **13**, 343-370.

Vichnevetsky, R., 1987: Wave propagation and reflection in irregular grids for hyperbolic equations. *Appl. Num. Math.*, **2**, 133-166.

Weisman, M.L., W.C. Skamarock, and J.B. Klemp, 1997: The resolution dependence of explicitly modeled convective systems. *Mon. Wea. Rev.*, **125**, 527-548.

Yakimiw, E., and A. Robert, 1990: Validation experiments for a nested grid-point regional forecast model. *Atmos.-Ocean*, **28**, 466-472.

Yanenko, N.N., 1971. *The Method of Fractional Steps*. Springer, New York.

Yessad, K., and P. Bénard, 1996: Introduction of a local mapping factor in the spectral part of the Météo France global variable mesh numerical forecast model. *Q. J. Roy. Meteor. Soc.*, **122**, 1701-1719.